International Conference on Mathematics, Computational Methods & Reactor Physics (M&C 2009)
Saratoga Springs, New York, May 3-7, 2009, on CD-ROM, American Nuclear Society, LaGrange Park, IL (2009)

AN EXTENSION OF THE GENERATION METHOD OF NON-NEGATIVE SCATTERING CROSS-SECTIONS FOR A TWO DIMENSIONAL GEOMETRY

Jong Woon Kim* and Young-Ouk Lee
Korea Atomic Energy Research Institute
150 Deokjin-dong, Yuseong-gu, Daejeon, 305-353, Korea
jwkim@kaeri.re.kr; yolee@kaeri.re.kr

Nam Zin Cho
Department of Nuclear and Quantum Engineering
Korea Advanced Institute of Science and Technology
373-1 Guseong-dong, Yuseong-gu, Daejeon, 305-701, Korea
nzcho@kaist.ac.kr

ABSTRACT

The differential scattering cross-sections in the discrete ordinates method are approximated as a truncated Legendre series. In the case of highly anisotropic scattering problems (e.g., incident beam problems), the prematurely truncated Legendre series give unphysical negative cross-sections for some values of μ (cosine of scattering angle). These unphysical artifacts cause negative scattering sources and negative angular fluxes. In addition, negative angular fluxes may lead to a wrong scalar flux as well. In this paper, the priority concept method to generate non-negative scattering cross-sections is extended to the X-Y geometry. The transport calculations are performed with P_6 Legendre scattering cross-sections and generated non-negative scattering cross-sections. To get the reference results, MCNP5 is used. The results show that the scalar fluxes with non-negative scattering cross-sections are much closer to the reference calculations without any unphysical negative angular fluxes.

Key Words: non-negative scattering cross-sections, X-Y geometry, Legendre expansion, anisotropic

1. INTRODUCTION

In solving the Boltzmann transport equation with the discrete ordinates method, the differential scattering cross-sections are approximated as a truncated Legendre series. In ENDF, the angular distribution of a scattering is expressed with high order expansions to have a non-negativity. However, the NJOY/TRANSX [1,2] code may have some difficulties to produce high-order (e.g., P_{20}) scattering matrix so that they generate prematurely truncated (e.g., P_6) scattering cross-sections even for the high energy range. In the case of high energy and highly anisotropic scattering problems (e.g., incident beam problems), the prematurely truncated Legendre scattering cross-sections give unphysical negative cross-sections for some values of μ . These

* Corresponding author, jwkim@kaeri.re.kr
Tel:+82-42-868-8795; FAX:+82-42-868-2636.

unphysical negative differential scattering cross-sections lead to negative scattering sources and negative angular fluxes even in the positive spatial difference (e.g., step difference) scheme.

Several methods have been proposed to avoid unphysical negative scattering cross-sections such as the Monte Carlo method [3] or numerical and closed-form integrations [4]. Recently, a deterministic method to generate non-negative scattering cross-sections was proposed for a one-dimensional geometry and the generated cross-sections were tested for the homogeneous slab transport problems [5]. This method uses conventional P_6 scattering cross-sections in the low energy range. However, in the high energy range where P_6 scattering cross-sections can not give an accurate angular distribution, the angular distribution of an elastic scattering in ENDF is used as a complementary data. The priority concept was applied to have a non-negativity based on the amount of contributions from the incoming direction to the other directions.

In this paper, we tested non-negative scattering cross-sections for the one-dimensional heterogeneous transport problem and extended the priority concept method for a two-dimensional geometry. The scalar fluxes were compared with the reference calculation and they show good agreements.

2. EXTENSION OF THE PRIORITY CONCEPT METHOD

2.1. Brief Introduction to the Priority Concept Method

The one-dimensional discrete ordinates equation [6] is

$$\mu_n \frac{d}{dz}\Psi_{g,n}(z)+\sigma_{t,g}(z)\Psi_{g,n}(z)=S_{g,n}+\frac{1}{k_{eff}}\chi_g\sum_{g'=1}^{G}\nu\sigma_{f,g'}(z)\Phi_{g'}(z)+S_{ext}, \tag{1}$$

where

$$S_{g,n}=\sum_{\ell=0}^{L}(2\ell+1)P_\ell(\mu_n)\sum_{g'=1}^{G}\sigma_{\ell,g,g'}(z)\Phi_{\ell,g'}(z), \tag{2}$$

$$\Phi_{\ell,g'}(z)=\frac{1}{2}\sum_{n'=1}^{N}w_{n'}P_\ell(\mu_{n'})\Psi_{g',n'}(z), \tag{3}$$

$$\Phi_g(z)=\frac{1}{2}\sum_{n=1}^{N}w_n\Psi_{g,n}(z), \quad \sum_{n=1}^{N}w_n=2. \tag{4}$$

To use the non-negative scattering cross-sections that are generated by the priority concept method, the scattering kernel in a discrete ordinates equation should be modified as:

$$S_{g,n}=\sum_{g'=1}^{G}\sum_{n'=1}^{N}\Delta\Omega_{n'}\,\overline{\sigma}^{non-negative}_{n'\to n,g'\to g}(z)\;\Psi_{g',n'}(z), \tag{5}$$

$$\Phi_g(z)=\frac{1}{4\pi}\sum_{n=1}^{N}\Delta\Omega_n\,\Psi_{g,n}(z), \tag{6}$$

$$\Delta\Omega_n=2\pi\,w_n, \quad \sum_{n=1}^{N}\Delta\Omega_n=4\pi, \tag{7}$$

where $\overline{\sigma}^{non-negative}_{n'\to n,g'\to g}(z)$ is a non-negative multi-group, average ordinate-to-ordinate scattering cross-sections (from energy group g' to g and ordinate n' to n) and this will be generated in a manner described below.

The main idea of this method is to make non-negative scattering cross-sections that produce equivalent scattering sources. Rewrite Eqs. (2) and (5) for group-to-group $(g'\to g)$ and ordinate-to-ordinate $(n'\to n)$ scatterings, we have

Legendre expansion:
$$S^{Le}_{n'\to n,g'\to g} = \sum_{\ell=0}^{L}(2\ell+1)P_\ell(\mu_n)\sigma_{\ell,g,g'}(z)\Phi_{\ell,g'}(z), \tag{8}$$

$$\Phi_{\ell,g'}(z) = \frac{1}{2}\sum_{n'=1}^{N} w_{n'}P_\ell(\mu_{n'})\Psi_{g',n'}(z), \tag{9}$$

New method:
$$S^{New}_{n'\to n,g'\to g} = \Delta\Omega_{n'}\,\overline{\sigma}^{non-negative}_{n'\to n,g'\to g}(z)\,\Psi_{g',n'}(z). \tag{10}$$

Calculate the scattering source with Eq. (8) in a condition that the incident angular flux, $\Psi_{g',n'=1}(z)$, is 1.0 and the others are zeros. The calculated scattering source, $S^{Le}_{n'=1\to n,g'\to g}$, represents the amount of scattering due to the unit angular flux incident from the ordinate $n'=1$. Repeat the calculation with incident ordinates $n'=1\ to\ N/2$. The scattering sources, $S^{Le}_{n'\to n,g'\to g}$, for $n'=N/2+1\ to\ N$ can be calculated with the results of $n'=1\ to\ N/2$ for the one-dimensional case. While calculating Eq. (8), if the P_6 scattering cross-section is not enough to represent an angular distribution of a scattering, the angular distribution of an elastic scattering in ENDF is used as a complementary data.

Set Eq. (8) to Eq. (10) in each group-to-group, ordinate-to-ordinate scattering to obtain,

$$S^{Le}_{n'\to n,g'\to g} \cong S^{New}_{n'\to n,g'\to g} = \Delta\Omega_{n'}\,\overline{\sigma}^{non-negative}_{n'\to n,g'\to g}(z)\,\Psi_{g',n'}(z), \tag{11}$$

and then we have $\overline{\sigma}^{non-negative}_{n'\to n,g'\to g}(z)$ as

$$\overline{\sigma}^{non-negative}_{n'\to n,g'\to g}(z) \cong \frac{S^{Le}_{n'\to n,g'\to g}}{\Delta\Omega_{n'}\,\Psi_{g',n'}(z)}, \tag{12}$$

where $\Psi_{g',n'}(z)$ is an angular flux for each incident group and ordinate.

The RHS of Eq. (12) is not non-negative, since $S^{Le}_{n'\to n,g'\to g}$ is calculated with a truncated Legendre expansion in Eq. (8). In such a case, we like to use a new notation $\overline{\sigma}_{n'\to n,g'\to g}(z)$ for the RHS of Eq. (12), where $\overline{\sigma}_{n'\to n,g'\to g}(z)$ is defined as

$$\bar{\sigma}_{n'\to n,g'\to g}(z) \equiv \frac{S^{Le}_{n'\to n,g'\to g}}{\Delta\Omega_{n'}\,\Psi_{g',n'}(z)}. \tag{13}$$

In order to have a non-negativity, we order each ordinate-to-ordinate scattering cross-section according to its magnitude at a given group-to-group transfer as

$$\bar{\sigma}^{k=1}_{n'\to n_{(k)},g'\to g}(z) > \bar{\sigma}^{k=2}_{n'\to n_{(k)},g'\to g}(z) > \cdots > \bar{\sigma}^{k=N}_{n'\to n_{(k)},g'\to g}(z), \tag{14}$$

where k is the priority index and N is the total number of ordinates.

The key idea of this procedure is that we set the high priority on the large and positive differential scattering cross-sections since it is a dominant contributor for the ordinate-to-ordinate $(n'\to n)$ scattering process at a given group-to-group transfer. However, the small or positive/negative oscillating ones are considered with a low priority.

According to the priority order, non-negative scattering cross-sections are assigned as follows:

$$\bar{\sigma}^{non-negative}_{n'\to n_{(k)},g'\to g}(z) = \begin{cases} \bar{\sigma}^{non-negative}_{n_{(k)}\to n',g'\to g}(z), & \mathrm{n_{(k)}} < \mathrm{n}', \quad (15)\\ \bar{\sigma}^{k}_{n'\to n_{(k)},g'\to g}(z), & \bar{\sigma}^{k}_{n'\to n_{(k)},g'\to g}(z) > 0, \quad (16)\\ \bar{\sigma}^{non-negative}_{n'\to n_{(k-1)},g'\to g}(z), & \bar{\sigma}^{k}_{n'\to n_{(k)},g'\to g}(z) \le 0. \quad (17) \end{cases}$$

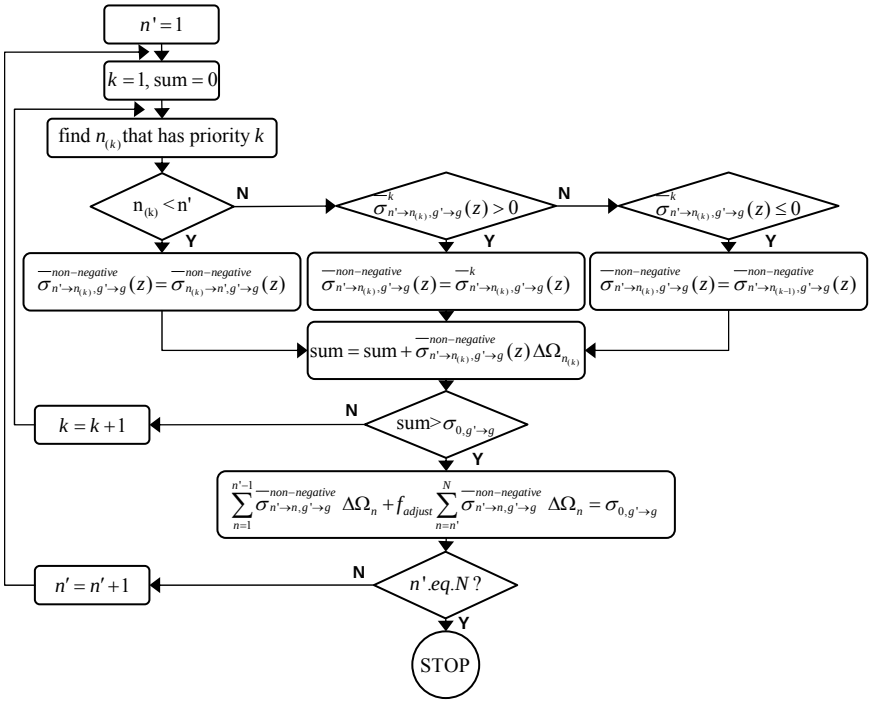

Figure 1. The flow chart of the assigning non-negative scattering cross-sections.

In order to conserve the 0th moment, we only adjust the assigned $\overline{\sigma}^{non-negative}_{n'\to n,g'\to g}(z)$ with Eqs. (16) and (17) as

$$\sum_{n=1}^{n'-1} \overline{\sigma}^{non-negative}_{n'\to n,g'\to g}\ \Delta\Omega_n + f_{adjust} \sum_{n=n'}^{N} \overline{\sigma}^{non-negative}_{n'\to n,g'\to g}\ \Delta\Omega_n = \sigma_{0,g'\to g}, \tag{18}$$

where $\sigma_{0,g'\to g}$ is the 0th moment of a macroscopic scattering cross-section from the TRANSX.

2.2. Extension of the Generating Non-Negative Scattering Cross-Sections for a Two-Dimensional Geometry

The extension of this method for a two-dimensional geometry is very easy and straight forward. The two-dimensional discrete ordinates equation is

$$\left[\mu_n \frac{\partial}{\partial x} + \eta_n \frac{\partial}{\partial y} + \sigma_{t,g}(\vec{r})\right] \Psi_g(\vec{r},\hat{\Omega}_n) = S_{g,n}(\vec{r}) + \frac{1}{k_{eff}} \chi_g \sum_{g'=1}^{G} \nu\sigma_{f,g'}(\vec{r})\, \Phi_{g'}(\vec{r}) + S_{ext}, \tag{19}$$

where

$$S_{g,n}(\vec{r}) = \sum_{\ell=0}^{L} \sum_{m=0}^{\ell} (2-\delta_{m,0}) Y^e_{\ell,m}(\hat{\Omega}_n) \sum_{g'=1}^{G} \sigma_{\ell,g,g'}\, \Phi^m_{\ell,g'}(\vec{r}), \tag{20}$$

$$\Phi^m_{\ell,g'}(\vec{r}) = \frac{1}{4} \sum_{n'=1}^{N(N+2)/2} w_{n'}\, Y^e_{\ell,m}(\hat{\Omega}_{n'}) \Psi_{g',n'}(\vec{r}), \tag{21}$$

$$\Phi_g(\vec{r}) = \frac{1}{4} \sum_{n=1}^{N(N+2)/2} w_n \Psi_{g,n}(\vec{r}), \qquad \sum_{n=1}^{N(N+2)/2} w_n = 4. \tag{22}$$

In this method, the following equations are used instead of Eqs. (20), (21), and (22):

$$S_{g,n}(\vec{r}) = \sum_{g'=1}^{G} \sum_{n'=1}^{N(N+2)/2} \Delta\Omega_{n'}\, \overline{\sigma}^{non-negative}_{n'\to n,g'\to g}(\vec{r})\ \Psi_{g',n'}(\vec{r}), \tag{23}$$

$$\Phi_g(\vec{r}) = \frac{1}{4} \sum_{n=1}^{N(N+2)/2} \Delta\Omega_n \Psi_{g,n}(\vec{r}), \tag{24}$$

$$\Delta\Omega_n = w_n, \qquad \sum_{n=1}^{N(N+2)/2} \Delta\Omega_n = 4. \tag{25}$$

The only difference between the one and two-dimensional cases is that the scattering sources are expressed with spherical harmonics like Eq. (20). When we use the priority concept method, the red dotted ordinates in Fig. 2 are only considered as incident ordinates due to the 1/8 symmetry.

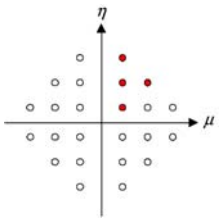

Figure 2. Illustration of the S_6 quadrature for a two-dimensional geometry.

3. NUMERICAL RESULTS

3.1. Non-Negative Scattering Cross-Sections

The generated non-negative scattering cross-sections for the one and two-dimensional geometries are compared with the conventional P_6 cross-sections data. The considered materials and details of the cross-section data are listed in Table I.

Table I. Details of the cross-section data

Basic Data	Processing Code	Cross-Sections Info.	Material
ENDF/B-VI	NJOY/TRANSX	P_6, 30 group (LANL-30)	H_2O ^{235}U

In the priority concept method, the angular distribution of the elastic scattering cross-sections in ENDF is used as complementary data to have an exact angular distribution of a scattering. The group index and the expansion order, L_{ENDF}, are listed in Table II.

Table II. Status of using the elastic scattering cross-sections as complementary data

Material	Energy groups for using elastic scattering cross-sections (energy group / L_{ENDF})
H_2O ^{235}U	- (1/20), (2/20), (3/20), (4/18), (5/18), (6/16), (7/14)

The non-negative scattering cross-sections obtained by the priority concept method are compared with the P_6 conventional truncated Legendre scattering cross-sections.

3.1.1. Application for a one-dimensional geometry

For the one-dimensional application, the S_{32} quadrature is used. The differential scattering cross-sections for H_2O and ^{235}U are shown in Fig. 3. The angular distribution with the priority concept method gives a good match without negative values.

In the Fig. 3.(b), three differential scattering cross-sections are compared. We can see that the P_6 expansion order is not high enough to accurately represent the angular distribution of within-group scattering cross-sections. However, the non-negative scattering cross-sections with the

priority concept method give fairly good angular distributions due to the complementary data without unphysical negative values.

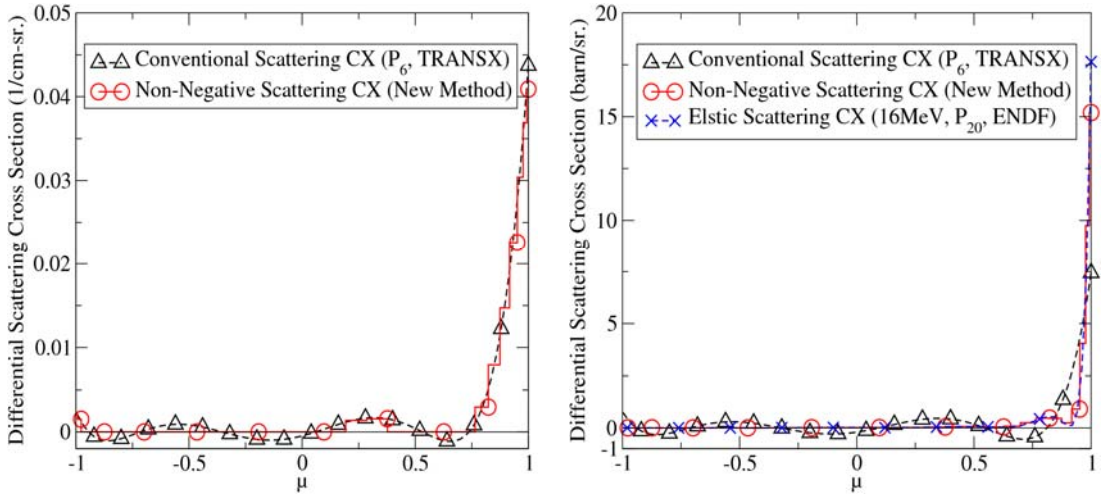

Figure 3. Differential scattering cross-sections for a one-dimensional geometry (S_{32}) ($g' = 1 \rightarrow g = 1$ and $n' = 1$): (a) H_2O; (b) ^{235}U.

3.1.2. Application for a two-dimensional geometry

Fig. 4 shows the ordinate-to-ordinate scattering cross-sections for H_2O. Figs. 4.(a) and 4.(b) are the ordinate-to-ordinate scattering cross-sections that are reproduced with the spherical harmonics based on the P_6 expansion. We can see a negative part of the cross-sections in some ordinates in Fig. 4.(b). However, in Fig. 4.(c), there are no unphysical negative ordinate-to-ordinate scattering cross-sections since they were generated with the priority concept method.

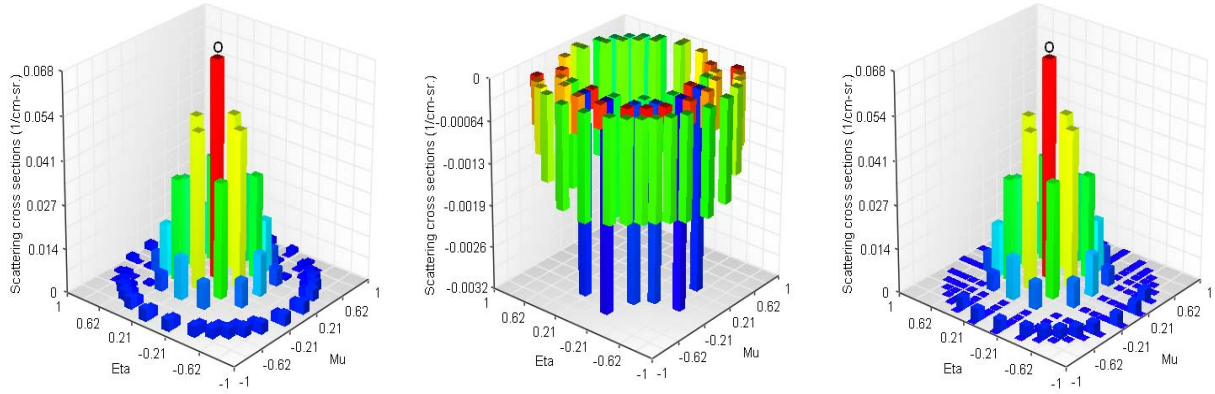

Figure 4. The within-group (1st group) differential scattering cross-sections of H_2O (S_{16}). The incident ordinate is marked with "O": (a) positive part of the cross-sections with spherical harmonics; (b) negative part of the cross-sections with spherical harmonics; (c) non-negative cross-sections with the priority concept method.

Fig. 5 shows the ordinate-to-ordinate scattering cross-sections for ^{235}U. Figs. 5.(a) and 5.(b) are the positive and negative parts of the scattering cross-sections that are reproduced. However, Fig. 5.(c) shows no unphysical negative scattering cross-sections. In addition, the angular distribution is very sharp compared to Fig. 5.(a) since the complementary data in the ENDF is used.

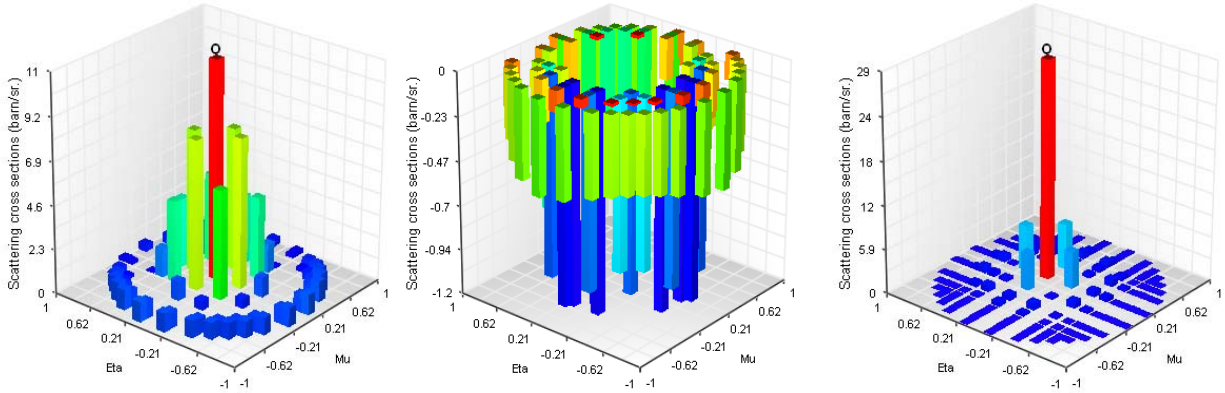

(a) **(b)** **(c)**

Figure 5. The within-group (1st group) differential scattering cross-sections of ^{235}U (S_{16}) and the incident ordinate is marked with "O": (a) positive part of the cross-sections with spherical harmonics; (b) negative part of the cross-sections with spherical harmonics; (c) non-negative cross-sections with the priority concept method.

3.2. Transport Calculations with Non-Negative Scattering Cross-Sections

3.2.1. Test problem I (one-dimensional heterogeneous)

The description of Test Problem I is shown in Fig. 6 and the calculation parameters are listed in Table III. The incident neutron beam is given in the first ordinate of the first group with strength 10 on the left boundary. In the calculation, the fission is considered as an absorption.

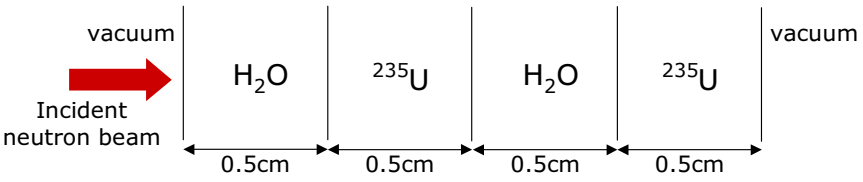

Figure 6. Configuration of Test Problem I.

Table III. The parameters for Test Problem I

Energy group	30 group (LANL-30)
Angular quadrature	S_{32}
Spatial mesh	200 meshes ($\Delta x = 0.01$cm)
Spatial differencing scheme	diamond difference (DD) scheme
Beam source	10/cm^2-sec given at the 1st ordinate, 1st group
Density	1.0 g/cm^3 for H_2O 19.1 g/cm^3 for ^{235}U
Error criterion	10^{-8}
Scattering cross-sections	Non-negative scattering cross-sections P_6 Legendre expansion

Fig. 7 shows the scalar fluxes of the first group. The two calculations give totally different results especially in the first and second slabs. The scalar flux that is calculated with the non-negative scattering cross-sections is much closer to the MCNP5 [7] result which is a reference.

This discrepancy can be explained with the detailed angular fluxes shown in Fig. 8. In Fig. 8.(a), the angular flux of the first ordinate match well with each other. However, in Fig. 8.(b), unphysical negative angular fluxes occurred all over the depth profile in the other ordinates. These unphysical negative angular fluxes cause the wrong scalar fluxes as shown in the Fig. 7.

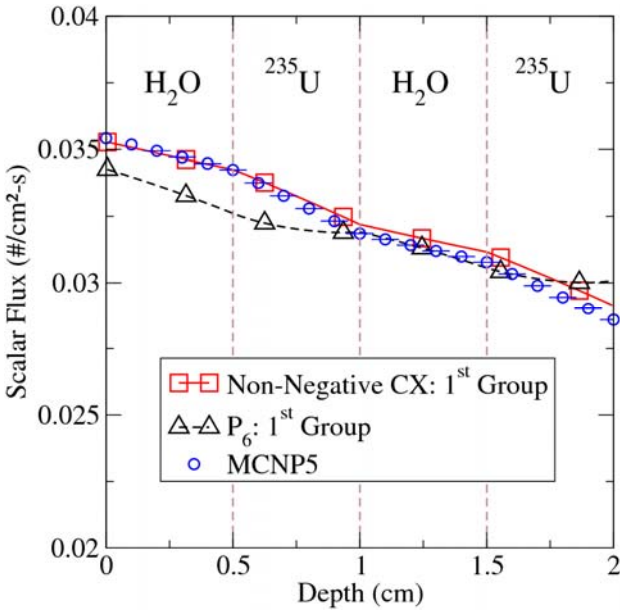

Figure 7. Comparison of the scalar fluxes (1st group, Test Problem I).

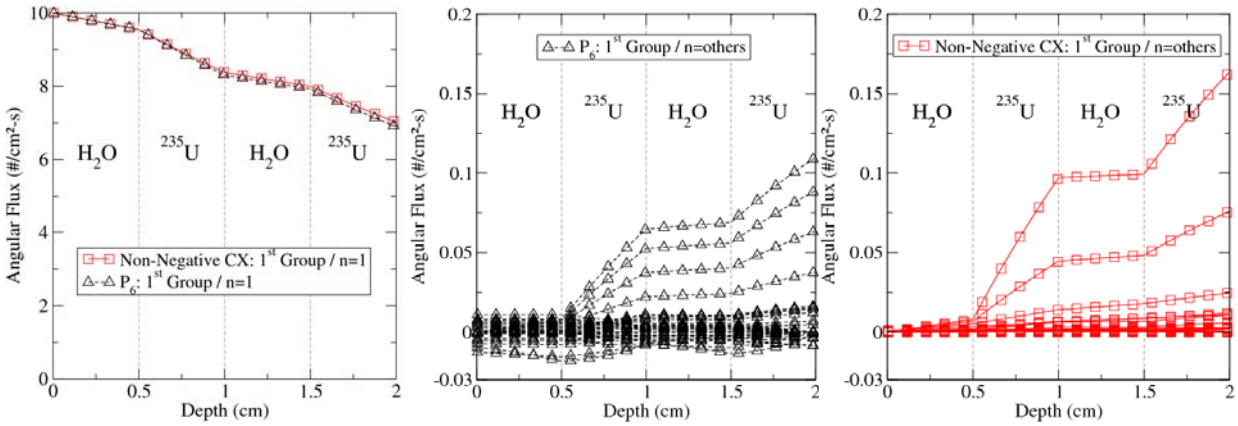

Figure 8. Comparison of the angular fluxes (1st group, Test Problem I): (a) 1st ordinate; (b) 2nd ~ 32th ordinates with the P_6 cross-sections; (c) 2nd ~ 32th ordinates with the non-negative scattering cross-sections.

3.2.2. Test problem II (two-dimensional heterogeneous)

The description of Test Problem II is shown in Fig. 9 and the calculation parameters are listed in Table IV. The incident neutron beam is given in the marked ordinates (in Fig. 9) of the first group with strength 10 on the left boundary. In the calculation, the fission is considered as an absorption.

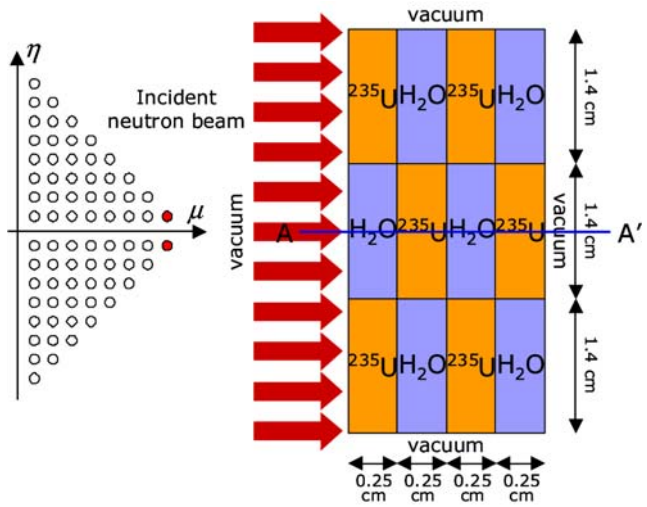

Figure 9. Configuration of Test Problem II.

Table IV. The parameters for Test Problem II

Energy group	30 group (LANL-30)
Angular quadrature	S_{16}
Spatial mesh	80 meshes ($\Delta x = 0.0125$cm) 75 meshes ($\Delta y = 0.056$cm)
Spatial differencing scheme	step difference (SD) scheme
Beam source	10/cm^2-sec given at the marked ordinates (in Fig. 9), 1st group
Density	1.0 g/cm^3 for H_2O 19.1 g/cm^3 for ^{235}U
Error criterion	10^{-8}
Scattering cross-sections	Non-negative scattering cross-sections P_6 Legendre expansion

Fig. 10 shows the scalar fluxes of the first group. Two scalar fluxes show a discrepancy and the scalar flux that is calculated with the non-negative scattering cross-sections is much closer to the MCNP5 reference result.

This discrepancy can be explained with the detailed angular fluxes shown in the Fig. 11. In the Fig. 11.(a), the angular fluxes where the beam is given match well with each other. However, in Fig. 11.(b), unphysical negative angular fluxes occurred in the other ordinates, even though the step difference scheme is used. These unphysical negative angular fluxes lead to the wrong scalar fluxes as shown in the Fig. 10.

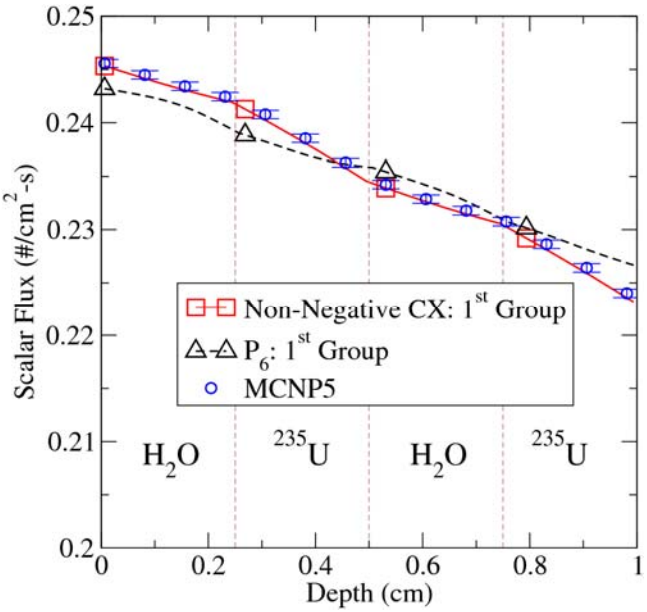

Figure 10. Comparison of the scalar fluxes along the A-A' (1st group, Test Problem II).

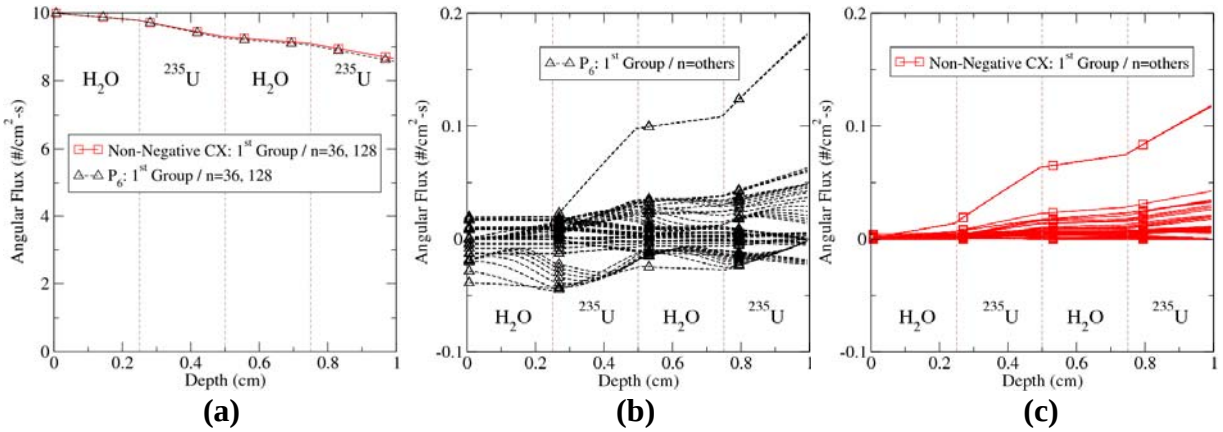

Figure 11. Comparison of the angular fluxes along A-A' (1st group, Test Problem II): (a) 36th and 128th ordinates; (b) other ordinates with the P_6 cross-sections; (c) other ordinates with the non-negative scattering cross-sections.

Fig. 12 shows the reference scalar flux that is tallied with MCNP5. Compare to the reference calculation, both results show large differences for the top and bottom edges compared to the other areas. Figs. 13.(a) and 13.(b) are the scalar flux differences compared to the reference result except for the top and bottom edges. As we can see clearly, the scalar flux with non-negative scattering cross-sections gives much better results than that with the P_6 cross-sections. The average scalar flux differences are calculated with

$$\left(\sum_{i=1}^{I} \sum_{j=1}^{J} \left| \Phi_{i,j,calculate} - \Phi_{i,j,MCNP} \right| \right) / (IJ), \tag{26}$$

and they are 2.105×10^{-3} and 1.252×10^{-3} where using the P_6 and non-negative cross-sections respectively.

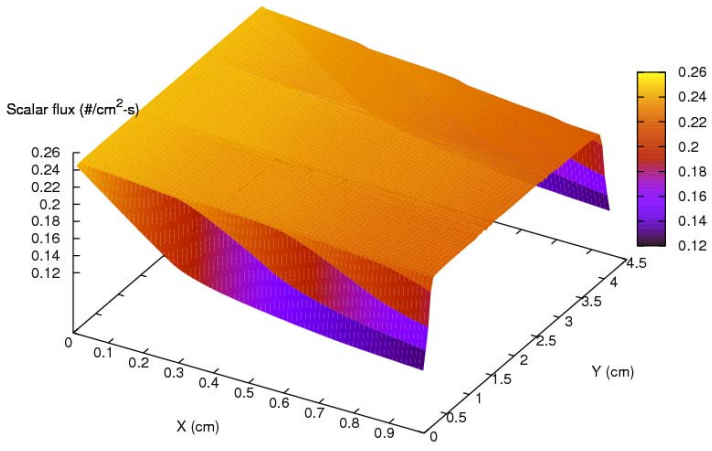

Figure 12. Reference scalar flux with MCNP5 (1st group, Test Problem II).

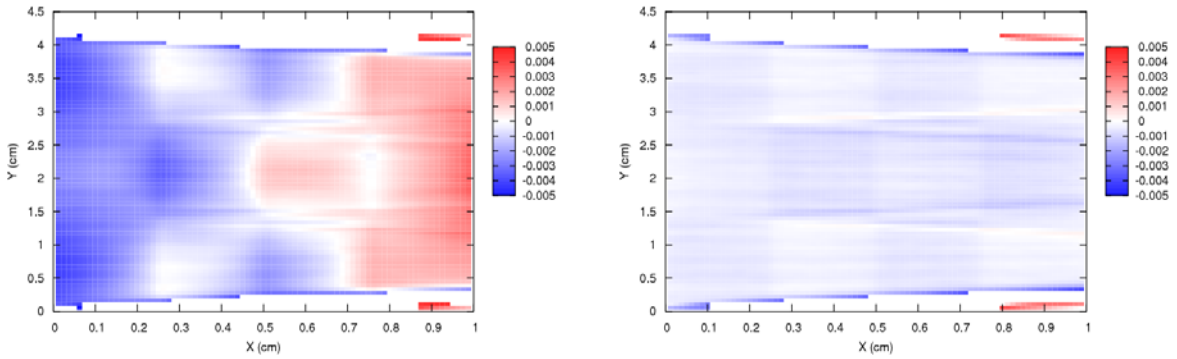

(a) **(b)**

Figure 13. The difference between each of the scalar fluxes compared to the reference calculation with MCNP5: (a) P_6 cross-section; (b) non-negative scattering cross-sections.

4. CONCLUSIONS

In this paper, the priority concept method to generate non-negative scattering cross-sections was introduced briefly and extended for a two-dimensional geometry. To elucidate its efficacy, non-negative scattering cross-sections were tested for one and two-dimensional heterogeneous transport problems. The results show that the scalar fluxes with the non-negative scattering cross-sections agreed well with the reference calculation without any unphysical negative angular fluxes.

ACKNOWLEDGMENTS

This work was carried out under the Institutional Activity Program of Korea Atomic Energy Research Institute.

REFERENCES

1. R.E. MacFarlane and D.W. Muir, *The NJOY Nuclear Data Processing System, Version 91*, LA-12740-M, Los Alamos National Laboratory (1994).
2. R.E. MacFarlane, *TRANSX 2: A Code for Interfacing MATXS Cross-Section Libraries to Nuclear Transport Codes*, LA-12312-MS, Los Alamos National Laboratory (1992).
3. J.M. DelGrande and K.A. Mathews, "Nonnegative Anisotropic Group Cross Sections: Hybrid Monte Carlo-Discrete Elements-Discrete Ordinates Approach," *Nucl. Sci. Eng.*, **139**, pp.33-46 (2001).
4. D.W. Gerts and K.A. Mathews, "Nonnegative Anisotropic Piecewise-Average Multigroup Cross Sections," *Nuclear Mathematical and Computational Sciences: A Century In Review – A Century Anew (M&C 2003),* Gatlinburg, Tennessee, April 6-10, on CD-ROM, (2003).
5. J.W. Kim and N.Z. Cho, "An Efficient Deterministic Method for Generating Non-Negative Scattering Cross-Sections," *Ann. Nucl. Energy,* **34**, pp.967-976 (2007).
6. E.E. Lewis and W.F. Miller Jr., *Computational Methods of Neutron Transport*, John Wiley & Sons, New York, U.S.A. (1984).
7. X-5 Monte Carlo Team, *MCNP – A General Monte Carlo N-Particle Transport Code, Version 5 Volume II: User's Guide*, LA-CP-03-0245, Los Alamos National Laboratory (2003).